HHS Public Access

Author manuscript

Anticancer Agents Med Chem. Author manuscript; available in PMC 2018 June 15.

Published in final edited form as:

Anticancer Agents Med Chem. 2017 ; 17(6): 813–820. doi:10.2174/1871520616666160923093959.

2-(ω-Carboxyethyl)pyrrole Antibody as a New Inhibitor of Tumor Angiogenesis and Growth

Chunying Wu[a,‡], **Xizhen Wang**[b,‡], **Nicholas Tomko**[c], **Junqing Zhu**[a], **William R. Wang**[d], **Jinle Zhu**[e], **Yanming Wang**[a,b,*], and **Robert G. Salomon**[c,*]

[a]Department of Radiology, Case Western Reserve University, 11100 Euclid Ave, Cleveland, OH 44106

[b]Department of Radiology, Bingzhou Medical University, Binzhou, Shandong, 256603

[c]Department of Chemistry, Case Western Reserve University, 11100 Euclid Ave, Cleveland, OH 44106

[d]Phillips Academy at Andover, 180 Main Street, Andover, MA 01810

[e]Beachwood High School, Beachwood, OH 44122

Abstract

Angiogenesis is a fundamental process in the progression, invasion, and metastasis of tumors. Therapeutic drugs such as Avastin and Lucentis have thus been developed to inhibit vascular endothelial growth factor (VEFG)-promoted angiogenesis. While these anti-angiogenic drugs have been commonly used in the treatment of cancer, patients often develop significant resistance that limits the efficacy of anti-VEGF therapies to a short period of time. This is in part due to the fact that an independent pathway of angiogenesis exists, which is mediated by 2-(ω-carboxyethyl)pyrrole (CEP) in a TLR2 receptor-dependent manner that can compensate for inhibition of the VEGF-mediated pathway. In this work, we evaluated a CEP antibody as a new tumor growth inhibitor that blocks CEP-induced angiogenesis. We first evaluated the effectiveness of a CEP antibody as a monotherapy to impede tumor growth in two human tumor xenograft models. We then determined the synergistic effects of Avastin and CEP antibody in a combination therapy, which demonstrated that blocking of the CEP-mediated pathway significantly enhanced the anti-angiogenic efficacy of Avastin in tumor growth inhibition indicating that CEP antibody is a promising chemotherapeutic drug. To facilitate potential translational studies of CEP-antibody, we also conducted longitudinal imaging studies and identified that FMISO-PET is a non-invasive imaging tool that can be used to quantitatively monitor the anti-angiogenic effects of CEP-antibody in the clinical setting. That treatment with CEP antibody induces hypoxia in tumor tissue was indicated by 43% higher uptake of [^{18}F]FMISO in CEP antibody-treated tumor xenografs than in the control PBS-treated littermates.

*Correspondence authors: Department of Chemistry and Radiology, Case Western Reserve University, Cleveland, OH 44106; yxw91@case.edu (YMW) and rgs@case.edu (RGS).

‡Equal contributions.

CONFLICT OF INTEREST

No potential conflicts of interest were disclosed

Keywords

Angiogenesis inhibitors; vascular endothelial growth factor (VEGF); Avastin; 2-(ω-carboxyethyl)pyrrole (CEP); positron emission tomography (PET); imaging

1. INTRODUCTION

Angiogenesis plays a critical role in tumor progression, invasion and metastasis.[1, 2] It has become an attractive molecular target for chemotherapy.[3] Anti-angiogenic tumor therapies focus on several regulatory and signaling molecules that control the process of formation and sprouting of new blood vessels. In particular, inhibition of vascular endothelial growth factor (VEGF) has shown antitumor activity in clinical settings, which results in starvation or apoptosis of tumor cells.[4] An example is Bevacizumab (Avastin) that is a monoclonal antibody that specifically recognizes and binds to VEGF-A.[5, 6] Avastin is currently approved by the U.S. Food and Drug Administration (FDA) as a first or second line therapeutic agent for treatment of glioblastoma and colorectal cancers (CRC), both of which are highly vascularized tumors that depend primarily on angiogensis.[7, 8]

Although Avastin monotherapy has been proven effective for several indications such as recurrent glioblastoma, many newly diagnosed cancer patients with glioblastoma do not respond and Avastin failed to provide a survival advantage.[9–12] The mechanism of intrinsic and acquired resistance to Avastin is not fully elucidated[13, 14], clinical investigations have suggested that other VEGF family members, including placental growth factor (PlGF), VEGF-C, VEGF-D [15–17], and cytokine angiogenic factors (CAFs)[18, 19], may modulate sensitivity to anti-VEGF-A (Avastin) therapy and allow regrowth of tumor-associated vasculature.[20–22] This is because Avastin blocks the main flow of blood, so tumors initially shrink, but the tumors may then switch dependence to other related growth factors in search of blood.[23] Additional examples of the complex refractory nature of VEGF to Avastin were discussed in a recent review.[24] Thus, additional angiogenesis pathways must exist that compensate for and contribute to resistance that develops to anti-VEGF-A therapy.

One alternative pathway promoting angiogenesis involves 2-(ω-carboxyethyl)pyrrole (CEP) derivatives of proteins and ethanolamine phospholipids that are generated by radical-induced oxidation of docosahexaenoate (DHA)-containing lipids.[25] CEP levels are elevated in ocular tissues from patients with age-related macular degeneration, as well as in human melanoma.[25–27] CEPs were shown to promote angiogenesis through a novel pathway. CEPs activate proangiogenic responses in a Toll-like receptor 2 (TLR-2)-dependant manner that is independent of VEGF receptors. This newly discovered angiogenesis pathway is anticipated to have great potential for the development of novel therapeutic interventions for cancer treatment. For example, by serving as a decoy receptor for CEP, a monoclonal CEP antibody could inhibit the TLR2-associated angiogenic signaling pathway synergistically with the monoclonal antibody Avastin that blocks the VEGF pathway by acting as a decoy receptor for VEGF. Previous studies demonstrated that treatment with anti-CEP mAb was effective in inhibiting tumor growth in a mouse allograft of melanoma. Concomitant inhibition of VEGF binding to VEGF-receptor (VEGF-R) further consolidated the tumor mass [25]. Thus, a

combination therapy, which inhibits angiogenesis by preventing activation of the CEP pathway, apparently can complement VEGF-R-based anti-angiogenesis therapy to significantly improve patient outcome.

For efficacy evaluation of a monoclonal CEP antibody therapy, it is important to identify an imaging technique that can provide a quantitative non-invasive measure of angiogenesis [28]. Molecular imaging for determining early responses of tumors to therapy is now very common in clinical practice. For example, [^{18}F]FDG-PET imaging is used routinely to assess the efficacy of cancer treatments. However, [^{18}F]FDG-PET reflects only metabolic changes, and the utility of [^{18}F]FDG for the assessment of therapy can be complicated by many other factors including surrounding tissue uptake, inflammation, body serum glucose level and other benign pathologies. Recent advances in molecular imaging technologies provide a means to non-invasively image the tumor microenvironment using positron emission tomography (PET). Used in combination with radiotracers, PET is a highly sensitive and specific imaging modality that can be used to monitor tumor environment. For example, [^{18}F]FDG PET is used routinely to assess the metabolic changes in the tumor tissue following chemotherapies. Hypoxia imaging may reflect changes in the tumor microenvironment after anti-angiogenic therapy. [^{18}F]fluoromisonidazole ([^{18}F]FMISO) is a proven hypoxia imaging probe[29, 30] that measures the hypoxia level in the microenvironment of the tumor following anti-angiogenic therapy [31]. We now report the application of PET imaging to determine tumor response to anti-CEP antibody therapy alone and to the combination therapy in xenograft models derived from glioblastoma and colorectal cancer cell lines.

As a prelude to translational studies, we conducted longitudinal studies in two human tumor xenograft models of colorectal cancer and glioblastoma comparing the efficacy of Avastin and CEP antibody in terms of tumor growth. Each tumor xenograft model was treated either with Avastin or CEP antibody and the tumor size was monitored over 24 days. We then examined the synergistic effects of Avastin and CEP antibody in the tumor xenograft model of glioblastoma through sequential treatment of Avastin followed by CEP antibody. In this longitudinal study, we first treated the xenografts with Avastin for 4 weeks followed by subsequent anti-CEP treatment for another 3 weeks. In addition, we also conducted [^{18}F]FDG- and [^{18}F]FMISO-PET imaging to determine which would be more responsive to CEP antibody therapy. Information from these studies is needed for future translational studies.

2. MATERIALS AND METHODS

Solvents and chemicals were purchased from Sigma-Aldrich unless stated otherwise. All chemicals obtained commercially were of analytic grade and used without further purification. Reference compound of [^{18}F]FMISO was purchased from ABX (Radeberg, Germany), [^{18}F]FDG was purchased from PETNET solution.

2.1. Radiosynthesis of [^{18}F]FMISO

The radiosynthesis of [^{18}F]FMISO was achieved in two steps in a TracerLab FXN automated synthesis module (GE Healthcare). Briefly, no-carrier-added ^{18}F-fluoride was

produced by the ^{18}O (p,n) ^{18}F nuclear reaction. Following nucleophilic fluorination with the tosylated precursor in the presence of kryptofix 222 (K_{222}) and K_2CO_3, the unreacted tosylate was removed by hydrolysis with hydrochloric acid. The reaction mixture was then neutralized with sodium hydroxide and sodium bicarbonate. The final product was purified by C-18 semi-preparative high performance liquid chromatography (HPLC, Phenomenex C-18 column, 10μ, 250 mm × 10 mm). Analytic HPLC was performed with a Raytest/ Angilent series 1100 HPLC (Phenomenex C-18 column, 5μ, 250 mm × 4.6 mm) system equipped with a UV detector and a Gabi radiodetector. [^{18}F] FMISO was produced with a high radiochemical purity (99%) and a specific activity of 1~2 Ci/mmol and was formulated in isotonic saline solution (pH 6.5–7.5), with a radioactivity concentration of 1.0~2.0 GBq/mL at the end of synthesis. The retention time of the radiolabeled [^{18}F]FMISO was identical to the retention time of the non-labeled FMISO as determined by ultraviolet detector under the same condition.

2.2. Preparation of colorectal and glioblastoma xenografts

All animal experiments were performed in accordance with a protocol conforming to Case Western Reserve University Institutional Animal Care and Use Committee (IACUC) guidelines. U87-MG (glioblastoma) and CRC 174 (LS174T, colorectal cancer) cell lines were purchased from American Type Culture Collection (ATCC). Briefly, a cell suspension was mixed with an equal volume of matrigel (BD Biosciences) to provide a cell concentration of 6 million cells/200uL, which was implanted subcutaneously into a 6–8 week-old female athymic nude mouse. Tumors were measured with a caliper or by CT imaging when the tumor volume reached approximately 200 mm^3. Mice were randomized into different groups for evaluation of therapeutic efficacy.

2.3. Dosing regimen

For tumor size measurement, Avastin (2.5mg/kg in 350uL sterile phosphate buffer solution, PBS) and murine monoclonal anti-CEP IgG^{32} (100μg in 350μL sterile PBS) were administered twice a week by intraperitoneal (i.p.) injection. Vehicle control was sterile PBS (350μl). For monotherapy treatment, mice were divided into three groups (5 per group): control PBS group (350 μL), Avastin group and anti-CEP antibody group. For combination therapy treatment, mice were divided into two groups. Both groups of mice were treated with Avastin until eventual therapeutic failure (the inception of exponential growth) at which point one group of mice was switched to anti-CEP therapy and for the other group of the mice Avastin was continued.

To monitor changes in the tumor environment during monotherapy in xenograft models, longitudinal [^{18}F]FMISO and [^{18}F] FDG microPET/CT imaging were performed before and after treatments. These mice were treated with Avastin and CEP antibody daily after the tumor size reached approximately 200 mm^3 (12 days after the xenografts were prepared) and imaged with [^{18}F]FMISO at day 0,2,4,8,10 and [^{18}F]FDG at day 0, 7 and 14, respectively.

2.4. Tumor Volume measurement

Throughout the study, the sizes of the tumors were either measured twice a week with a caliper or every other day with CT. When measured with calipers, the volume of a tumor

was calculated with the equation [(A×B×C)]×0.523[33], where A is the longest measurement, B is the shortest measurement, and C is the highest measurement. Once the tumor volume reached approximately 200 mm^3, mice were randomized into different groups for evaluation of therapeutic efficacy.

2.5. *In vivo* microPET/CT imaging

PET imaging of [^{18}F]FMISO and [^{18}F]FDG were performed using a Siemens (Erlangen, Germany) Inveon microPET/CT scanner. For anatomic localization, both a PET image and a CT image were subsequently acquired for co-registration. Prior to PET imaging, CT scout views were taken to ensure that tumors were placed in the co-scan field of view (FOV) where the highest image resolution and sensitivity were achieved. Each group of mice was administered through lateral tail vein injection with a solution of [^{18}F]FDG or [^{18}F]FMISO (150~200 μCi in 0.2ml saline). The animals were imaged under isoflurane anesthesia (2% in oxygen), and biologic monitoring for respiration and temperature was performed with a BioVet system (m2m imaging). For [^{18}F]FDG PET imaging, animals were fasted overnight prior to imaging with access only to water. Their diet was then replenished after imaging. The mice were statically imaged with either [^{18}F]FMISO at 90~110min after injection or with [^{18}F]FDG at 40~60min after injection. After PET data acquisition, a low-dose CT scan was performed for anatomic registration and attenuation correction. The microPET images obtained were reconstructed using a two-dimensional ordered-subset expectation maximum (OSEM) algorithm. PET and CT data were analyzed with Carimas software provided by the Turku PET Centre. For quantitative analysis, the co-registered microPET/CT images were used to accurately define the region of interest (ROI) and quantify the radioactivity concentrations in the tumor region in terms of standardized uptake values (SUV). For comparison, SUV of each mouse was normalized to its baseline scan. Tumor volumes were calculated in terms of mm^3 using the Carimas software.

2.6. *In vitro* immunohistochemistry staining

At the end of the experiments, tumors were removed and postfixed by immersion in 4% paraformaldehyde (PFA) overnight, dehydrated in 30% sucrose solution, embedded in freezing optimal cutting temperature (OCT) compound, Fisher Scientific, Suwanee, GA), cryostat sectioned at 10 μm on a microtome and mounted on superfrost slides (Fisher Scientific). These tumor slices were subjected to CD31 immunohistochemistry staining. Generally, after being blocked with blocking buffer (5% bovine serum albumin, 2.5% fetal calf serum, and 0.4% triton-100) for 30 min, the frozen sections were incubated with primary antibody (rat anti-mouse CD31, 1:100, BD bioscience) for 2 hours at room temperature followed by storing at 4 °C overnight. The secondary antibody (anti-mouse Alexa Fluro 568, 1:800, Invitrogen) was then added and incubated for another 1 hour at 37 °C. After washing with PBST (3 × 5 min), the slides were covered with VECTASHIEID mount media with 4′,6-diamidino-2-phenylindole (DAPI). Images were collected using a Nikon fluorescence microscope.

2.7. Statistical analysis

Quantitative data were expressed as mean ± SEM, and statistical significance of observed differences among different experimental groups was calculated using a two-tailed student t test. p values <0.05 were considered to be statistically significant.

3. RESULTS

3.1. CEP antibody treatment inhibited tumor growth in colorectal and glioblastoma tumor xenograft models

We evaluated the antitumor activity of CEP antibody in comparison with Avastin in both human colorectal and human glioblastoma tumor xenografts that were prepared by subcutaneous injection of LS174T and U87-MG tumor cell lines, respectively, into the flanks of athymic nude mice. For each tumor xenograft model, the animals were randomly assigned to 3 groups for anti-CEP, Avastin and PBS treatment. After the tumor size reached 200 mm^3 (day 12 after xenografts), each group was treated with CEP antibody, Avastin, or PBS twice a week.

As shown in Figure 1, both CEP antibody and Avastin showed similar antitumor effects in both xenograft models. The tumor sizes were monitored over 25 days and compared with vehicle treated controls. For the LS174T human colorectal tumor-bearing xenografts, CEP antibody treatment showed an average tumor growth rate of 18% while Avastin treatment showed 15% (Figure 1A). This was a significant reduction of 16.3% when compared with the vehicle-treated control littermates, which showed 31.2%. For U87-MG glioblastoma tumor-bearing mice, anti-CEP antibody and Avastin were administered intraperitoneally every other day. As shown in Figure 1B, an even more profound inhibition of tumor growth was found in the glioblastoma tumor-bearing xenografts. The tumor size did not increase and remained practically the same over the 25 days when treated with either CEP antibody or Avastin. Compared to the PBS treated control littermates, the average tumor growth rate was reduced by 33.2%.

Following the imaging studies, we then examined the extent of angiogenesis in the tumor tissues through histochemistry using anti-CD31 that is a specific marker of newly formed blood vessels. At the end of the experiments, mice bearing LS174T tumor were euthanized and the tumor tissues were dissected and sectioned for CD31 staining. The extent of newly formed vasculature was then compared among the three treatment groups. As shown in Figure 2A–C, the LS174T tumors treated only with PBS showed abundant vasculature, as indicated by strong CD31 staining. In comparison, the LS174T tumors treated with Avastin showed much less CD31 staining, suggesting angiogenesis was significantly reduced (Figure 2D–F). More importantly, CEP antibody could even further reduce the extent of angiogenesis as CEP-antibody-treated tumor tissue sections showed the least CD31 staining among the three treatment groups (Figure 2G–I). Significant reduction of CD31 staining supports the conclusion that CEP antibody effectively inhibits the formation of new blood vessels that halts or delays tumor growth as previously monitored (Figure 1).

3.2. Sequential treatment with Avastin and then CEP antibody further inhibited glioblastoma tumor growth

Because Avastin and anti-CEP inhibit tumor growth through two independent pathways with different mechanisms, we hypothesized that growth of a tumor resistant to Avastin could still be responsive to anti-CEP, which inhibits tumor growth in a TLR-2–dependent manner without activation of VEGFR-1 and VEGFR-2 [25]. To test this hypothesis, we evaluated the synergistic effect of Avastin and CEP antibody. Thus mice bearing U87-MG glioblastoma cells were first prepared. At day 9 when solid tumor tissues are palpable, the xenografts were treated with Avastin (2.5 mg/kg) alone twice a week for 18 days until drug resistance had developed and the tumors resumed growing (Figure 3). At this point, the xenografts were divided into two groups, one group was subjected to continued treatment with Avastin (2.5 mg/kg) alone and the other group was subjected to treatment with Avastin combined with anti-CEP (1:1, 5 mg/kg) twice a week. During the first phase of treatment, the tumors in all the xenografts grew very slowly until day 27, when drug resistance to Avastin treatment had developed. During the second phase of treatment after Avastin started failing, we observed significantly enhanced growth inhibition by CEP antibody when administered in combination with Avastin. Compared to Avastin therapy alone, the average tumor size was reduced by 28.9% by the end of the experiment. These studies suggested that CEP antibody did independently block the tumor growth promoted through a pathway that compensates for inhibition of the VEGF-mediated pathway by Avastin.

3.3. Non-invasive imaging for efficacy evaluation of anti-CEP treatment

The above studies demonstrated the potential of CEP-antibody as a therapeutic drug that can be used either by itself or in combination with Avastin to inhibit tumor growth. For future translational studies, an imaging marker must be identified that allows for quantitative assessment of anti-CEP treatment with high sensitivity and specificity. Thus, we evaluated [^{18}F]FDG- and [^{18}F]FMISO-PET to determine which technique would be more responsive to anti-CEP treatment.

[^{18}F]FDG PET imaging is commonly used for assessing the effects of chemotherapy on glucose metabolism in the tumor. To determine if [^{18}F]FDG-PET correlates with tumor growth, we conducted longitudinal imaging in LS174T tumor xenografts that were treated with CEP antibody twice a week starting from day 12 after xenografts. [^{18}F] FDG PET scans were acquired at day 0, 7 and 14 following anti-CEP treatment. As shown in Figure 4, [^{18}F]FDG uptake in the tumor tissues showed a weak correlation (PBS: $r^2 = 0.001941$, anti-CEP: $r^2 = 0.2767$) with the tumor growth rate observed previously. After normalizing to day 0 and comparing with the control PBS group, we only observed reduction of [^{18}F]FDG uptake at day 7 after treatments. However, [^{18}F]FDG uptake was increased at later time points (i.e., at day 14). Overall, no significant differences were observed between the treated and control groups. Interestingly, PET images of the control tumors showed reduced [^{18}F]FDG uptake in the center of the tumor tissue due to the exponential tumor growth and subsequent necrosis.

On the other hand, solid tumors often develop hypoxia during their evolution. This is primarily caused by unregulated cellular growth, resulting in a greater demand on oxygen

for energy metabolism [34]. As a consequence, most solid tumors evolve their own tissue physiological microenvironment, which is largely dictated by abnormal vasculature and metabolism. Recently [^{18}F]FMISO was developed for PET imaging of hypoxia, which was designed to detect the changes in the tumor microenvironment after anti-angiogenic therapy [34]. We thus conducted [^{18}F]FMISO PET imaging of the LS174T human colorectal tumor xenografts to determine if [^{18}F]FMISO PET correlated with the efficacy of anti-CEP treatment. After the xenografts were treated with CEP antibody, [^{18}F]FMISO PET scans were acquired every other day. As shown in Figure 5, uptake of [^{18}F]FMISO in tumor tissue increased over time and correlated well with tumor growth ($r^2 = 0.9016$). When normalized to day 0 and compared with the control PBS group (poor correlation, $r^2 = 0.109$), we observed significant differences over a period of 10 days after anti-CEP treatment. [^{18}F]FMISO uptake in CEP-antibody treated tumor xenografs was 42.8% higher than that in the control littermates, suggesting that CEP antibody induced hypoxia in the tumor tissue.

4. DISCUSSION

Inhibition of angiogenesis is a major therapeutic strategy for halting tumor growth in cancer. FDA-approved drugs that inhibit VEGF-promoted angiogenesis such as Avastin and Lucentis have been thoroughly investigated and widely used in the clinic with moderate success. Most anti-VEGF therapies exhibit limited efficacy just for a few months before drug resistance is developed. This led us to hypothesize that multiple pathways exist that compensate each other in promoting vascularization during tumor growth. Our basic research on lipid oxidation led to the discovery that oxidatively truncated docosahexaenoate phospholipids convert primary amino groups of biomolecules into 2-(ω-carboxyethyl)pyrrole (CEP) derivatives, which accumulate under inflammatory conditions inherent in cancer as well as age-related macular degeneration (AMD). Further studies showed that CEPs promote angiogenesis through a novel VEGF-independent TLR2-dependent pathway. As shown in Figure 6, signaling through TLR2 and VEGF apparently mediates two independent pathways that promote angiogenesis leading to tumor growth, which may compensate for each other and contribute to the development of drug resistance to single therapy alone. Therefore, synergistic inhibition of both angiogenesis pathways, e.g., using the corresponding monoclonal antibodies as decoy receptors, has the potential to improve patient response and clinical outcomes.

For this reason, we evaluated an anti-CEP antibody as a potential monoclonal antibody therapy. We first evaluated the efficacy of the anti-CEP antibody for inhibition of tumor growth in two different human tumor xenografts prepared from the LS174T colorectal cancer cell line and a glioblastoma cancer cell line. Each group of xenografts (n = 5) was treated separately with anti-CEP antibody, Avastin, and PBS alone for three weeks. The tumor size was monitored longitudinally (Figure 1). Compared to PBS control, both treatment groups exhibited much slower tumor growth rates. Both anti-CEP and Avastin significantly inhibited tumor growth. Unlike the PBS-treated controls, the anti-CEP and Avastin-treated tumor xenografts exhibited no exponential phase of tumor growth at later time points. Immunohistological analysis of tumor tissues indicated that much less new vasculature was formed after anti-CEP or Avastin treatments (Figure 2), which confirms that the slower tumor growth is associated with inhibition of angiogenesis. These studies showed

that anti-CEP is similarly effective as Avastin in both types of xenografts, further suggesting that TLR2- and VEGF-mediated pathways are indeed independent from each other in angiogenesis and can be modulated separately.

In the clinic, patients undergoing Avastin therapy alone often develop drug resistance that limits its efficacy to a few months. In glioblastoma, for example, essentially all patients develop recurrent or progressive disease after initial therapy. Various clinical trials indicated that Avastin has proven effective for recurrent glioblastoma for a short period of time. Continuous Avastin treatment, however, often fails to halt the tumor growth, leading to generally poor clinical outcomes with a median overall survival of only 3.8 months. It is thus critical to develop a combination therapy that can prevent the exponential tumor regrowth immediately after Avastin fails. For this reason, we explored the synergistic effects of Avastin and anti-CEP antibody. A cohort of glioblastoma tumor xenografts was treated first with Avastin for 3 weeks. Then, the xenografts were randomly divided into two groups, one was further treated with Avastin and the other was treated with anti-CEP antibody. As shown in Figure 3, the xenografts undergoing continuous treatment of Avastin readily entered the second phase of steady exponential tumor growth, suggesting these xenografts had developed drug resistance against Avastin. However, when the previous Avastin-treated xenografts were sequentially treated with anti-CEP antibody, the exponential growth phase was slightly retarded. These studies demonstrated the synergistic effects of Avastin and anti-CEP antibody in inhibiting angiogenesis. To our best knowledge, this is the first combination therapy that has ever been developed that could potentially overcome drug resistance of VEGF-targeted anti-angiogenesis therapy.

To facilitate future clinical trials of such combination therapy in patients, it is important to identify an effective imaging modality that allows for longitudinal monitoring not only tumor size but also the extent of angiogenesis with high sensitivity and specificity. Because anti-angiogenic therapies often lead to consolidation of tumor mass instead of regression, the standard volumetric measurement is not a sensitive approach and the tumor response is often underestimated. For this reason, we focused on positron emission tomography (PET), which is a functional imaging technique widely used in the clinic that allows for directly monitoring of targets affected by chemotherapies. Because anti-angiogenesis treatment would eventually affect the energy consumption and oxygen supply conditions in the tumor, we conducted PET imaging using either [^{18}F]FDG to monitor glucose metabolism rate or [^{18}F]FMISO) to assess tumor hypoxia. These imaging studies were expected to enhance our understanding of the biological consequences of CEP monoclonal antibody therapy and of the value of each radiotracer as an imaging marker for non-invasive assessment of efficacy.

As shown in Figure 4, the energy consumption in terms of FDG uptake in the colorectal tumor was quantified following anti-CEP antibody treatment. Compared to PBS-treated controls, anti-CEP treated tumor xenografts exhibited little and insignificant reduction of FDG uptake. This can perhaps be explained by the fact that energy consumption is a global indicator of tumor growth and may not directly correlate to vascularization. Because vascularization would directly affect oxygen supply conditions in the tumor, a hypoxia imaging marker such as FMISO may be more sensitive than FDG. Indeed, our longitudinal imaging studies using FMISO-PET showed a significant difference between anti-CEP

treated tumors and PBS-treated controls. Quantitative analysis suggested that anti-CEP treatment led to increased uptake of FMISO over time, while little or no change was observed in PBS-treated controls. Now that FMISO-PET has been used in patients similar like FDG-PET, use of such PET imaging would greatly facilitate future clinical trials to evaluate the efficacy of anti-CEP therapy.

5. CONCLUSION

Through the above studies, we demonstrated that a CEP antibody is a potential therapeutic agent that can delay tumor growth by inhibiting angiogenesis and diminishing vascularization. This involves a new CEP mediated TLR2-dependent pathway that is independent of the VEGF pathway, making it possible to develop combination therapy that would enhance the efficacy of anti-angiogensis. Our studies also indicate that once tumor resistance to Avastin occurs, administration of anti-CEP therapy can be of great benefit. Meanwhile, the angiogenetic effect of CEP antibody can also be non-invasively monitored by [^{18}F]FMISO-PET imaging, which showed a superior correlation compared to [^{18}F]FDG. These preclinical studies should be helpful in accelerating anticancer drug development and promoting the clinical translation of molecular imaging by providing a platform on which the efficacy of various combinations of chemotherapeutic agents can be optimized.

Acknowledgments

This work was supported by grants GM021249-33 and -34 (to R. G. Salomon) and GM021249-33S1 and -34S1 (to R. G. Salomon and Y. Wang) from the National Institutes of General Medical Studies of the National Institutes of Health.

LIST OF ABBREVIATIONS

VEGF	vascular endothelial growth factor
CEP	2-(ω-carboxyethyl)pyrrole
TLR-2	Toll-like receptor 2
PET	positron emission tomography
[^{18}F]FMISO	1H-1-(3-[^{18}F]-fluoro-2-hydroxy-propyl)-2-nitro-imidazole
CAF	cytokine angiogenic factors
PlGF	placental growth factor
OSEM	ordered-subset expectation maximum
SUV	standardized uptake values
ROI	region of interest
PFA	paraformaldehyde
OCT	optimal cutting temperature

DAPI 4′,6-diamidino-2-phenylindole

References

1. Chung AS, Lee J, Ferrara N. Targeting the tumour vasculature: insights from physiological angiogenesis. Nat Rev Cancer. 2010; 10(7):505–14. [PubMed: 20574450]
2. Ferrara N, Kerbel RS. Angiogenesis as a therapeutic target. Nature. 2005; 438(7070):967–74. [PubMed: 16355214]
3. Carmeliet P, Jain RK. Molecular mechanisms and clinical applications of angiogenesis. Nature. 2011; 473(7347):298–307. [PubMed: 21593862]
4. Folkman J. Tumor angiogenesis: therapeutic implications. N Engl J Med. 1971; 285(21):1182–6. [PubMed: 4938153]
5. Shih T, Lindley C. Bevacizumab: an angiogenesis inhibitor for the treatment of solid malignancies. Clin Ther. 2006; 28(11):1779–802. [PubMed: 17212999]
6. Jain RK, Duda DG, Clark JW, Loeffler JS. Lessons from phase III clinical trials on anti-VEGF therapy for cancer. Nat Clin Pract Oncol. 2006; 3(1):24–40. [PubMed: 16407877]
7. Deborah Huveldt LJL-T, Carlson Brett L, Schroeder Mark A, Rodriguez Fausto, Giannini Caterina, Galanis Evanthia, Sarkaria Jann N, Anastasiadis Panos Z. Targeting Src Family Kinase Inhibitor Bevacizumab-induced *Glioa Cell Invasion*. PLoS One. 2013; 8(2)
8. Saltz LB, Clarke S, Diaz-Rubio E, Scheithauer W, Figer A, Wong R, et al. Bevacizumab in combination with oxaliplatin-based chemotherapy as first-line therapy in metastatic colorectal cancer: a randomized phase III study. J Clin Oncol. 2008; 26(12):2013–9. [PubMed: 18421054]
9. Dawson SJ, Conus NM, Toner GC, Raleigh JM, Hicks RJ, McArthur G, et al. Sustained clinical responses to tyrosine kinase inhibitor sunitinib in thyroid carcinoma. Anticancer Drugs. 2008; 19(5):547–52. [PubMed: 18418222]
10. Scott BJ, Quant EC, McNamara MB, Ryg PA, Batchelor TT, Wen PY. Bevacizumab salvage therapy following progression in high-grade glioma patients treated with VEGF receptor tyrosine kinase inhibitors. Neuro Oncol. 2010; 12(6):603–7. [PubMed: 20156808]
11. Yuasa T, Takahashi S, Hatake K, Yonese J, Fukui I. Biomarkers to predict response to sunitinib therapy and prognosis in metastatic renal cell cancer. Cancer Sci. 2011; 102(11):1949–57. [PubMed: 21812860]
12. Gilbert MR, Dignam JJ, Armstrong TS, Wefel JS, Blumenthal DT, Vogelbaum MA, et al. A randomized trial of bevacizumab for newly diagnosed glioblastoma. N Engl J Med. 2014; 370(8): 699–708. [PubMed: 24552317]
13. Mesange P, Poindessous V, Sabbah M, Escargueil AE, de Gramont A, Larsen AK. Intrinsic bevacizumab resistance is associated with prolonged activation of autocrine VEGF signaling and hypoxia tolerance in colorectal cancer cells and can be overcome by nintedanib, a small molecule angiokinase inhibitor. Oncotarget. 2014; 5(13):4709–21. [PubMed: 25015210]
14. Gokmen-Polar Y, Goswami CP, Toroni RA, Sanders KL, Mehta R, Sirimalle U, et al. Gene Expression Analysis Reveals Distinct Pathways of Resistance to Bevacizumab in Xenograft Models of Human ER-Positive Breast Cancer. J Cancer. 2014; 5(8):633–45. [PubMed: 25157274]
15. Cao R, Eriksson A, Kubo H, Alitalo K, Cao Y, Thyberg J. Comparative evaluation of FGF-2-, VEGF-A-, and VEGF-C-induced angiogenesis, lymphangiogenesis, vascular fenestrations, and permeability. Circulation research. 2004; 94(5):664–70. [PubMed: 14739162]
16. Hindryckx P, Waeytens A, Laukens D, Peeters H, Van Huysse J, Ferdinande L, et al. Absence of placental growth factor blocks dextran sodium sulfate-induced colonic mucosal angiogenesis, increases mucosal hypoxia and aggravates acute colonic injury. Lab Invest. 2010; 90(4):566–76. [PubMed: 20142801]
17. Hamdollah Zadeh MA, Amin EM, Hoareau-Aveilla C, Domingo E, Symonds KE, Ye X, et al. Alternative splicing of TIA-1 in human colon cancer regulates VEGF isoform expression, angiogenesis, tumour growth and bevacizumab resistance. Mol Oncol. 2014; doi: 10.1016/j.molonc.2014.07.017
18. Kopetz S, Hoff PM, Morris JS, Wolff RA, Eng C, Glover KY, et al. Phase II trial of infusional fluorouracil, irinotecan, and bevacizumab for metastatic colorectal cancer: efficacy and circulating

angiogenic biomarkers associated with therapeutic resistance. J Clin Oncol. 2010; 28(3):453–9. [PubMed: 20008624]

19. Willett CG, Duda DG, di Tomaso E, Boucher Y, Ancukiewicz M, Sahani DV, et al. Efficacy, safety, and biomarkers of neoadjuvant bevacizumab, radiation therapy, and fluorouracil in rectal cancer: a multidisciplinary phase II study. J Clin Oncol. 2009; 27(18):3020–6. [PubMed: 19470921]
20. Batchelor TT, Sorensen AG, di Tomaso E, Zhang WT, Duda DG, Cohen KS, et al. AZD2171, a pan-VEGF receptor tyrosine kinase inhibitor, normalizes tumor vasculature and alleviates edema in glioblastoma patients. Cancer cell. 2007; 11(1):83–95. [PubMed: 17222792]
21. Casanovas O, Hicklin DJ, Bergers G, Hanahan D. Drug resistance by evasion of antiangiogenic targeting of VEGF signaling in late-stage pancreatic islet tumors. Cancer Cell. 2005; 8(4):299–309. [PubMed: 16226705]
22. Kerbel RS. Therapeutic implications of intrinsic or induced angiogenic growth factor redundancy in tumors revealed. Cancer cell. 2005; 8(4):269–71. [PubMed: 16226701]
23. Lieu CH, Tran H, Jiang ZQ, Mao M, Overman MJ, Lin E, et al. The association of alternate VEGF ligands with resistance to anti-VEGF therapy in metastatic colorectal cancer. PLoS One. 2013; 8(10):e77117. [PubMed: 24143206]
24. Claesson-Welsh L. Blood vessels as targets in tumor therapy. Upsala. J Med Sci. 2012; 117(2): 178–86.
25. West XZ, Malinin NL, Merkulova AA, Tischenko M, Kerr BA, Borden EC, et al. Oxidative stress induces angiogenesis by activating TLR2 with novel endogenous ligands. Nature. 2010; 467(7318):972–6. [PubMed: 20927103]
26. Wang H, Guo J, West XZ, Bid HK, Lu L, Hong L, Jang GF, Zhang L, Crabb JW, Clinical G, Linetsky M, Salomon RG. Proteomic AMDSG. Detection and biological activities of carboxyethylpyrrole ethanolamine phospholipids (CEP-EPs). Chem Res Tox. 2014; 27(12):2015–22.
27. Kutralanathan Renganathan JG, Rayborn Mary E, Crabb John S, Robert G, Salomon RJC, Kapin Michael A, Romano Carmelo, Hollyfield Joe G, Crabb W. CEP Biomarkers as Potential Tools for Monitoring Therapeutics. PLoS One. 2013; 8(10):13.
28. Oehler C, O'Donoghue JA, Russell J, Zanzonico P, Lorenzen S, Ling CC, et al. 18F-fluromisonidazole PET imaging as a biomarker for the response to 5,6-dimethylxanthenone-4-acetic acid in colorectal xenograft tumors. J Nucl Med. 2011; 52(3):437–44. [PubMed: 21321262]
29. Cher LM, Murone C, Lawrentschuk N, Ramdave S, Papenfuss A, Hannah A, et al. Correlation of hypoxic cell fraction and angiogenesis with glucose metabolic rate in gliomas using 18F-fluoromisonidazole, 18F-FDG PET, and immunohistochemical studies. J Nucl Med. 2006; 47(3): 410–8. [PubMed: 16513609]
30. Koh WJ, Bergman KS, Rasey JS, Peterson LM, Evans ML, Graham MM, et al. Evaluation of oxygenation status during fractionated radiotherapy in human nonsmall cell lung cancers using [F-18]fluoromisonidazole positron emission tomography. Int J Rad Oncol Biol Phys. 1995; 33(2): 391–8.
31. Murakami M, Zhao S, Zhao Y, Chowdhury NF, Yu W, Nishijima K, et al. Evaluation of changes in the tumor microenvironment after sorafenib therapy by sequential histology and 18F-fluoromisonidazole hypoxia imaging in renal cell carcinoma. Int J Oncol. 2012; 41(5):1593–600. [PubMed: 22965141]
32. Cui, Y. PhD Thesis. Case Western Reserve University; 2014. Design, Development, and Production of Therapeutic Immunoglobulins for Inhibition of Carboxyethylpyrrole-Induced Angiogenesis.
33. Kumar K, Wigfield S, Gee HE, Devlin CM, Singleton D, Li JL, et al. Dichloroacetate reverses the hypoxic adaptation to bevacizumab and enhances its antitumor effects in mouse xenografts. J Mol Med (Berl). 2013; 91(6):749–58. [PubMed: 23361368]
34. Rajendran JG, Krohn KA. Imaging hypoxia and angiogenesis in tumors. Radiol Clin North Am. 2005; 43(1):169–87. [PubMed: 15693655]

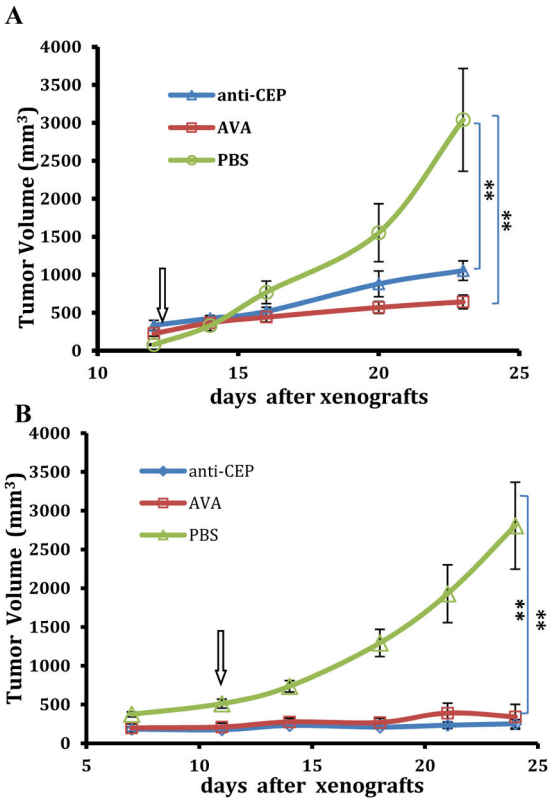

Figure 1.

Antitumor activity of anti-CEP antibody in LS174T colorectal cancer models (A) and glioblastoma tumor models (B) compared with Avastin and control vehicle. A: Mice were treated with anti-CEP antibody (100 μg in a total of 350 μl of PBS), Avastin (100 μg in a total of 350 μl of PBS) and PBS (350 μl) daily at 12 days after xenografts. The tumor sizes were measured by CT imaging using Carimas software. B: Mice were treated with anti-CEP antibody (100 μg in a total of 350 μl of PBS), Avastin (100 μg in a total of 350 μl of PBS) and PBS twice a week at 12 days after xenografts. The tumor sizes were measured by calipers. Arrows denote the day when treatment of anti-CEP, Avastin and PBS were initiated. Data were expressed as mean ± SEM, n = 5. Double asterisk (**) $P<0.05$.

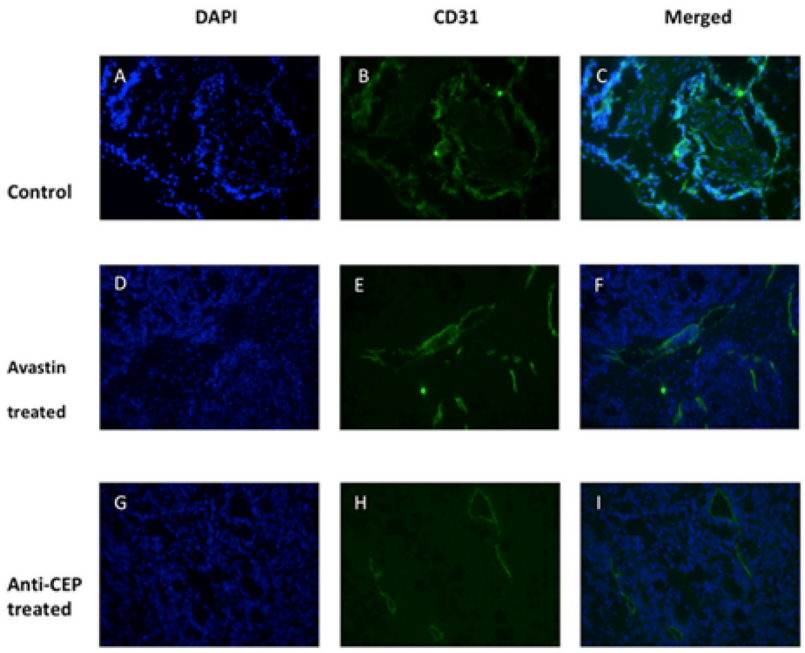

Figure 2.

Angiogenesis represented by immunofluorescence CD31 staining in LS174T tumors. Representative sections were taken from Avastin, anti-CEP and vehicle treated LS174T tumors at the end of the experiment. Significantly decreased CD31 staining and changes of vascular morphology between the treated group and the control group were observed.

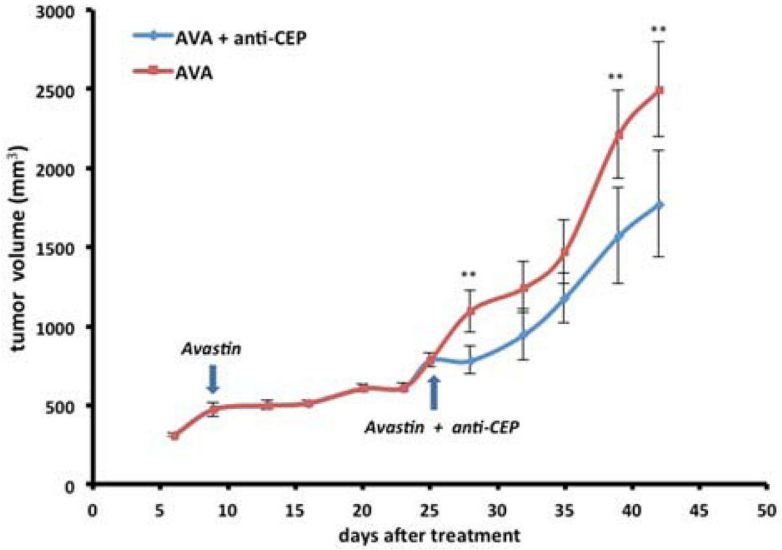

Figure 3.

Tumor growth of U87-MG bearing nude mice *in vivo* treated with Avastin only started from day 6 and combination treatment (Avastin started at day 9 and anti-CEP started at day 27) to the end of the experiment. The tumor sizes were measured by calipers. Arrows denote the day when treatment of Avastin and anti-CEP were initiated. Data were expressed as mean ± SEM, n = 10. Double asterisk (**) $P<0.05$.

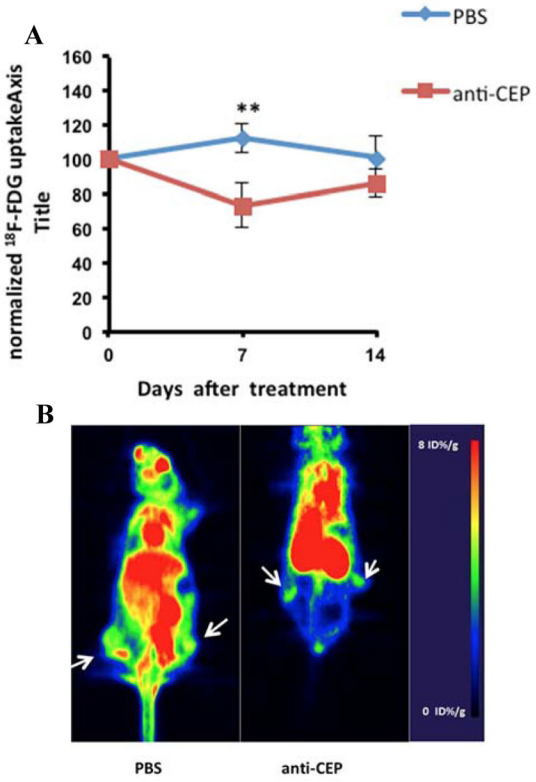

Figure 4.

In vivo uptake of ^{18}F-FDG in LS174T colorectal tumors in PBS and anti-CEP treated animals. A: quantitative analysis of tumor uptake normalized to baseline scan at day 0. Data were expressed as mean ± SEM, n = 5. Double asterisk (**) $P<0.05$. B: representative PET images of ^{18}F-FDG uptake in PBS and anti-CEP treated animals at day 7. Arrows denote location of the tumors.

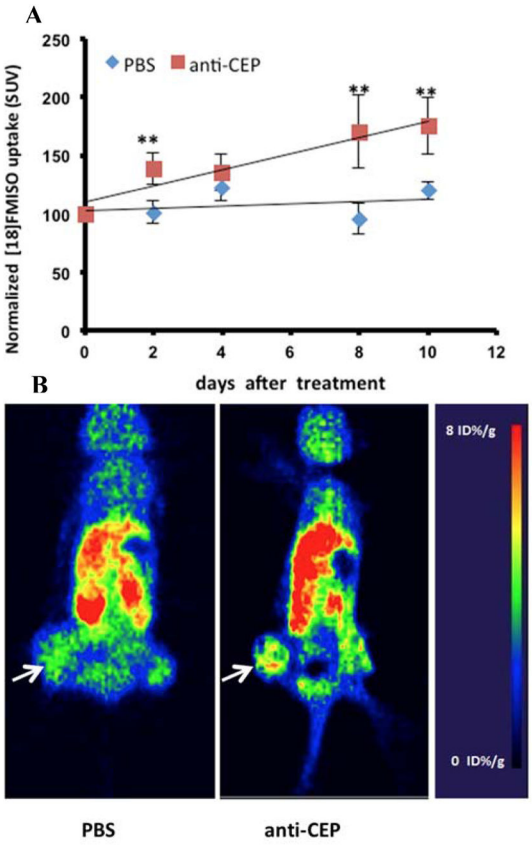

Figure 5.

In vivo uptake of ^{18}F-FMISO in LS174T colorectal tumors in PBS and anti-CEP treated animals. A: quantitative analysis of tumor uptake of ^{18}F-FMISO normalized to baseline scan at day 0. Data were expressed as mean ± SEM, n = 5. Double asterisk (**) P<0.05. B: representative PET images of ^{18}F-FMISO uptake in PBS and anti-CEP treated animals at day 2 after treatment. Arrows denote where tumors are., normalized to baseline scan at day 0. Data were expressed as mean ± SEM, n = 5. Double asterisk (**) P<0.05.

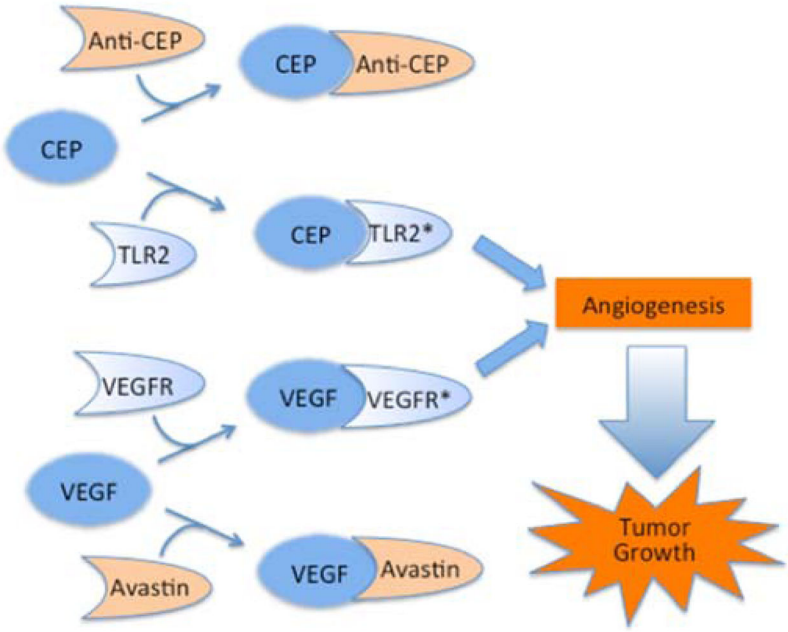

Figure 6.

TLR2 and VEGFR dependent pathways independently promote angiogenesis and tumor growth that can be inhibited by a monoclonal anti-CEP antibody and the anti-VEGF monoclonal antibody Avastin respectively.